

Review Article

Nanoporous Aluminium Oxide Membranes as Cell Interfaces

Dorothea Brüggemann

Max Planck Institute for Intelligent Systems, Heisenbergstrasse 3, 70569 Stuttgart, Germany

Correspondence should be addressed to Dorothea Brüggemann; brueggemann@physik.rwth-aachen.de

Received 23 November 2012; Accepted 4 January 2013

Academic Editor: Alexandru Vlad

Copyright © 2013 Dorothea Brüggemann. This is an open access article distributed under the Creative Commons Attribution License, which permits unrestricted use, distribution, and reproduction in any medium, provided the original work is properly cited.

Nanoporous anodic aluminium oxide (AAO) has become increasingly important in biomedical applications over the past years due to its biocompatibility, increased surface area, and the possibility to tailor this nanomaterial with a wide range of surface modifications. AAO nanopores are formed in an inexpensive anodisation process of pure aluminium, which results in the self-assembly of highly ordered, vertical nanochannels with well-controllable pore diameters, depths, and interpore distances. Because of these outstanding properties AAO nanopores have become excellent candidates as nanostructured substrates for cell-interface studies. In this comprehensive review previous surveys on cell adhesion and proliferation on different AAO nanopore geometries and surface modifications are highlighted and summarised tabularly. Future applications of nanoporous alumina membranes in biotechnology and medicine are also outlined, for instance, the use of nanoporous AAO as implant modifications, coculture substrates, or immunoisolation devices.

1. Introduction

Nanoporous biointerfaces are a fast emerging field in current nanomaterials research. Over the past years, the development of novel biomedical applications has benefited immensely from the unique properties of nanoporous anodic alumina oxide (AAO) membranes [1, 2]. Alumina membranes are a class of self-organized, highly ordered, and biocompatible nanomaterials with regular pore size, uniform pore density and high porosity over a large scale, thus providing an increased surface area [1]. Over and above, nanoporous AAO is optically transparent, electrically insulating, chemically stable, bioinert, and biocompatible [3]. These outstanding properties are beneficial for various applications of AAO membranes in biotechnology and medicine ranging from biofiltration membranes [4–6], lipid bilayer support structures [7], biosensing devices [8–12], and implant coatings [13–16] to drug delivery systems with AAO capsules [3, 17–19] and scaffolds for tissue engineering [20–23]. Furthermore, AAO nanopores are not always used on their own. They

also serve as widely used template for other biocompatible nanostructures such as gold and platinum nanopillars [24–26].

The vertical alumina nanochannels with cylindrical shape are produced from aluminium films or membranes using a very efficient and low-cost anodisation process with polyprotic acids, for example, oxalic, phosphoric, or sulphuric acid. The formation of the straight nanopores in this procedure has been studied extensively and is highly reproducible by choosing specific anodisation parameters such as temperature and pH value of the acid bath or the anodisation voltage [27–29]. Moreover, the electrochemical production of biocompatible AAO templates is often combined with prestructuring approaches such as electron beam lithography to create localized nanostructures in the nanoporous templates [30–32]. The surface of AAO nanopores can also be modified with versatile methods to tailor them for specific cell growth. In addition, nanoporous AAO membranes have a low-background autofluorescence, which is advantageous for cell counting applications in particular [33]. Because of

these outstanding biomaterial properties nanoporous AAO membranes have gained increasing interest as cell-interface substrates for manifold cell types and biomedical applications. Since several years, this nanomaterial is also available in commercial form, thus providing ease of use in cell culture studies. A widely spread product with pore sizes from 20 to 200 nm is AnoporeTM/AnodiscTM from Whatman (supplied by GE Healthcare or SPI Technologies, US). AAO membranes with diameters ranging from 13 to 150 nm are currently fabricated by Synkera Technologies (US), and nanoporous AAO cell culture chips with up to 180000 micron-sized growth compartments are produced by Microdish in The Netherlands.

Since nanotopographic features of a biomaterial such as nanoporous AAO influence its interaction with biological tissues or cells [22, 34], I here review recent studies on the growth of various cell types on nanoporous AAO. I will discuss neuronal cell growth, connective tissue cell cultures, epithelial cell cultures, muscle cells and blood cells as well as microorganisms on AAO nanopores. An overview on the various studies on different cell types cultivated on AAO membranes is composed in Table I. Customised AAO nanopores have been used in these surveys as well as commercially available alumina membranes and different coatings and surface modifications were employed. Furthermore, versatile biomedical applications employing AAO nanopores will be highlighted in this paper, ranging from implant coatings and coculture substrates to drug-delivery capsules and various surface modifications of nanoporous AAO membranes.

2. Neuronal Cell Cultures on Nanoporous AAO Membranes

In various studies, AAO membranes have already been used as substrates for neuronal cell cultures with the prospect of developing advanced neural implants and sensing devices. Haq et al. investigated the neurite development in pheochromocytoma (PC12 cells) by culturing them on gold-coated AAO membranes having pore sizes comparable to filopodia (around 200 nm) [35]. For 4 days in culture they found a limited neurite outgrowth and the formation of shorter neurites on gold-coated nanoporous AAO than on smooth coverslip references. This observation led them to the assumption that PC12 cells were spatially sensing the underlying nanotopography by responding in different neurite outgrowth activities. However, the authors assume that the ridges of the nanopores still provide a limited support for the movement of the filopodia and the growth cones. This result may suggest that AAO nanotopographies can be used to control neurite outgrowth in neuronal cell cultures, for instance, to find an application as neural implant.

The pitch-dependence of AAO membranes on the neurite outgrowth of primary hippocampal neurons was studied by Cho et al. using four different AAO nanotopographies [36]. They distinguished between AAO substrates with different pitch size and distinct pore depth. Their study focussed on the first two days of cell culture because the nanotopographical effect is mainly expressed in the early stage of cell culture.

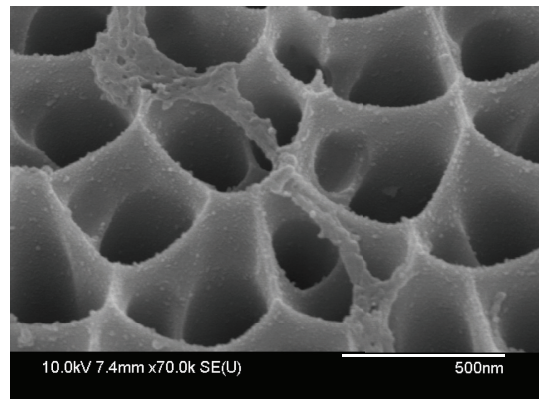


FIGURE 1: Morphological features of neurite outgrowth on a nanoporous AAO substrate with 400 nm pitch after 2 days in culture [36].

Axon outgrowth was observed to be faster on substrates with a 400 nm pitch than on nanopores with a 60 nm pitch. For 400 nm pitch size, they also found an accelerated axon outgrowth, which started earlier and was accompanied by the formation of longer neurites (see Figure 1). In their study, the depth of the pores was not found to have any effect on the neurite growth. The authors therefore concluded that the neurites mostly responded to the pitch of the nanotopographies and that this knowledge will be beneficial to tailor future neuronal biointerfaces with AAO.

The neuronal cell growth on AAO membranes has also been investigated with regard to possible biosensing applications. Wolfrum et al. developed AAO membranes on silicon substrates as neuronal biohybrid interface. The interpore distances in this study ranged from 30 to 200 nm. Primary rat embryonic cortical neurons on polylysine coating and locust thoracic ganglia neurons on concanavalin A-coating were cultured on AAO up to 14 days. Both neuronal cell types adhered and proliferated well on the AAO nanopores during this time, and no dependence of the electrophysiological performance of the cells on the underlying substrate was found [37]. Furthermore, the cell environment of the neuronal cultures on the nanopores could be controlled with small amounts of chemicals, and it was possible to address the cells highly localized through the AAO nanopores. A future perspective will be to integrate these nanoporous on-chip membranes into sensing or stimulation devices to combine high-resolution electrical and chemical interfaces on a single chip, for instance, to create an artificial chemical synapse.

Recently, CMOS electrodes have been modified with nanoporous AAO membranes of different pitch sizes (see Figure 2) to create an interface of optimum pore morphology with mammalian neuronal cells (NG108-15) [38, 39]. In these studies, the AAO membrane also served as a corrosion inhibitor, thus enhancing the lifetime of the electrodes. For large pore pitches of 206 nm, an improved neuronal adhesion was observed with slightly better performance than on the planar aluminium surface of unmodified CMOS electrodes. However, small-pore pitches of 17 nm and 69 nm resulted in low cell adhesion. Hence, porous alumina with larger pitch

TABLE 1: Overview on the various cell types, which have been cultured on nanoporous AAO substrates with versatile geometries.

	Cell type	AAO nanopore geometry	Cell growth promoting coating	Reference
Neuronal cell cultures	Rat pheochromocytoma (PC12)	(i) Commercial AAO membranes (Anodisc, Whatman International Ltd) with pore diameters around 200 nm (ii) Gold coating of 50 nm	Self-assembled monolayer cysteamine and poly-L-lysine	[35]
	Primary hippocampal neurons	Customised AAO membranes: (i) Pitch sizes from 60 to 450 nm (ii) Pore depth varying from flat to nanoporous substrates	N-(2-aminoethyl)-3-aminopropyltrimethoxysilane	[36]
	Primary rat embryonic cortical neurons and locust thoracic ganglia neurons	Customised AAO nanopores: (i) Interpore distances of 20 to 300 nm (ii) Porosity up to 40%	(i) Polylysine for rat neurons (ii) Concanavalin A for insect neurons	[37]
	Mammalian neuronal cells (NG108-15)	Customised alumina nanopores on CMOS electrodes, produced with two-step anodisation: pitch sizes of 17 to 206 nm	N/A	[38, 39]
Connective tissue cell cultures	Primary hippocampal neurons	Customised AAO membranes embedded in silicon: diameters from 25 to 100 nm	Poly-L-lysine	[40]
	Human osteoblast-like cells (HOB)	Customised nanoporous AAO on titanium substrates: pore sizes from 160 to 200 nm	N/A	[13, 14]
		Commercial Anodisc membranes (Whatman) with 200 nm pore size	N/A	[41]
	Human osteosarcoma cell line (MG63)	Customised alumina nanopores on titanium sheets and commercial Anodiscs (Whatman): pore sizes ranging from 20 to 200 nm	Coating: N/A Pores were partially filled with silica nanoparticles.	[42]
Primary bone marrow stromal cells (MSCs)	Human fetal osteoblasts (hFOB 1.19)	Customised AAO nanopores on aluminium sheets, produced by two-step anodisation: pore diameters between 75 and 89 nm. Anodiscs with 20 to 200 nm pores (Whatman) used as reference	N/A	[43, 44]
		Customised alumina nanopores on aluminium sheets, prepared in a two-step anodisation process: pore diameters of 30 to 80 nm	Vitronectin followed by arginine-glycine-aspartic acid-cysteine (RGDC)	[45]
		Customised AAO membranes, produced by two-step anodisation of aluminium sheets: 72 nm pore size	N/A	[46]
NIH 3T3 fibroblasts		Customised AAO membranes with pore sizes ranging from 40 to 500 nm and commercial 200 nm Anodisc nanopores (Whatman)	N/A	[20]
		(i) Customised AAO nanopores with diameters from 75 to 300 nm. (ii) A mask of PDMS holes was also deposited on the AAO membranes	N/A	[47]

TABLE 1: Continued.

Cell type	AAO nanopore geometry	Cell growth promoting coating	Reference
Murine 3T3 fibroblasts	(i) Commercial Anodisc membranes with 200 nm pores (Whatman) were coated with a polyethylene glycol hydrogel (PEG) (ii) Using photolithography microcompartments were produced in the PEG layer with sizes from $50 \times 50 \mu\text{m}^2$ to $200 \times 200 \mu\text{m}^2$ and 10 um high walls	Cell adhesive peptide Gly-Arg-Gly-Asp-Ser (GRGDS)	[48]
IMR-90 lung fibroblasts	(i) Customised nanoporous AAO biocapsules with pores of 75 nm, prepared by two-step anodisation (ii) PEG modification on the outer surface of the AAO capsule	N/A	[49]
Epithelial cells	Human embryonic kidney cells (HEK293) Human mammary epithelial cells (HMEC) Human vascular endothelial cells from the umbilical cord (ECV304) Human cervix carcinoma cell line (HeLa) Human KYSE-30 esophageal squamous epithelial cancer cells HaCaT keratinocytes Human epidermal keratinocytes	Customised AAO nanopores (i) Interpore distances of 20 to 300 nm (ii) Porosity up to 40% Customised AAO membranes, prepared in a two-step anodisation: (i) Pore diameter variation: 30, 40, 45, 50, and 80 nm (ii) Variation of pore depth for a constant pore diameter of 80 nm: depths of 50, 90, 130, 180, 240, and 300 nm Customised AAO nanopores, prepared in a two-step anodisation: (i) Pore diameters of 50 and 200 nm (ii) Pore depths of 500 and 2000 nm (i) Commercial AAO tissue culture inserts with pore sizes of 20 nm (Nunc, Thermo Fisher) (ii) AAO membrane was supported by a perforated PDMS film and placed between two electrodes to enable local electrical stimulation and solute delivery (i) Customised AAO nanopores produced via two-step anodisation (25 to 75 nm) (ii) Structuring PEG coating via photolithography yielded circular microcompartments with diameters of 80 to 500 μm . Customised AAO membranes with pore sizes ranging from 40 to 500 nm and commercial 200 nm Anodisc membranes (Whatman) (i) Commercial Anodisc membranes with 20 nm pores (Whatman) (ii) ALD coating with 8 nm Pt (i) Commercial Anodisc nanopores with 20 and 100 nm diameter (Whatman) (ii) ALD coating with 8 nm TiO_2	Extracellular matrix gel N/A N/A [37] [50] N/A [51] N/A Fibronectin Fibronectin [52] [53] Fibronectin N/A 1-Mercaptoundec-11-yl hexa(ethylene glycol) monolayers N/A [11, 54] [20] [55] [56]

TABLE 1: Continued.

Cell type	AAO nanopore geometry	Cell growth promoting coating	Reference	
Hepatoma cell line HepG2	Customised nanoporous AAO membranes: (i) Self-supported AAO substrates with 40 and 270 nm diameter (ii) Mechanically stabilized AAO membranes with 63 and 234 nm pore size	N/A	[34, 57–59]	
Primary mouse hepatocytes, cocultured with human adipose-derived mesenchymal stem cells (hASCs)	Customised, self-supported AAO membranes with pore sizes ranging from 50 to 60 nm	N/A	[60]	
Pancreatic cell line MIN6	Customised nanoporous AAO biocapsules with pore sizes between 46 and 75 nm, prepared by two-step anodisation	MIN6 cells were embedded into a collagen matrix inside the AAO capsule	[61]	
Human retinal endothelial cells (HREC)	Commercial alumina membrane cell culture inserts (Nunc, Fisher Scientific) with 20 nm pore size	N/A	[62]	
Muscle cells	<p>Mouse smooth muscle cells</p> <p>Murine C2C12 myotubes</p> <p>Cardiomyocyte HL-1 cells</p>	<p>Commercial nanoporous Anodisc membranes with 20 nm and 200 nm pore diameters (Whatman)</p> <p>(i) Commercial nanoporous alumina membrane culture inserts with pores of 20 nm (Nunc, Thermo Fisher) (ii) AAO membrane was supported by a perforated PDMS film to create an electroporation device</p> <p>(i) Customised AAO nanopores with diameters below 50 nm (ii) AAO nanopores as cell interface on gold microelectrode array</p>	<p>N/A</p> <p>BD MatrigelTM solution (BD Biosciences) containing ECM proteins Atelocollagen coating for muscle tissue-like stiffness</p> <p>Fibronectin and gelatin</p>	[63]
Blood cells	<p>Neutrophils</p> <p>Monocytes and macrophages</p> <p>Human platelet rich plasma</p> <p>Whole blood</p>	<p>Commercial nanoporous Anodisc alumina membranes (Whatman): pore diameters of 20 and 200 nm</p> <p>Commercial Anodisc nanopores (Whatman) with pore diameters of 20 and 200 nm</p> <p>(i) Commercial nanopores with 20 nm diameter (Whatman) (ii) ALD coating with 8 nm Pt</p> <p>Commercial Anodisc nanopores (Whatman) with pore sizes of 20 and 200 nm</p>	<p>No coating</p> <p>Protein coating (human serum, collagen type I, fibronectin, bovine serum albumin)</p> <p>No coating</p> <p>1-Mercaptoundec-11-yl hexa(ethylene glycol) monolayers</p> <p>Blood collection materials were coated with heparin. AAO nanopores remained uncoated</p>	[67]
			[68]	
			[69]	
			[55]	
			[70–74]	

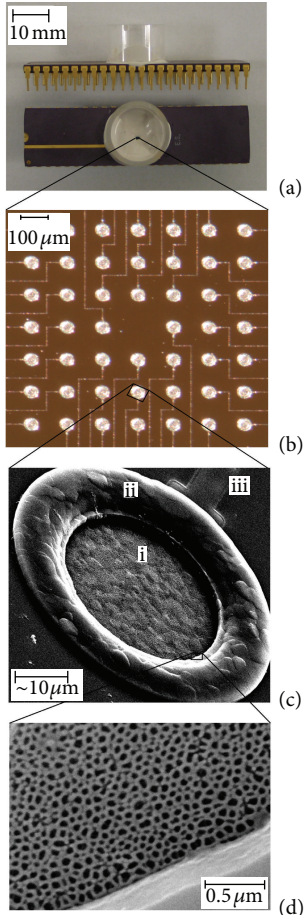


FIGURE 2: Anodising of CMOS pad: (a) assembled device with culture chamber and exposed electrode array, (b) array of 48 electrode pads, (c) SEM image of a single pad, tilted by 55°: (i) electrode surface, (ii) passivation rising over outer edge of metal, (iii) metal track connection, and (d) an anodised pad (30 V, 4% phosphoric acid, 22°C) with passivation at lower right [39].

sizes can be used to improve the performance of low-cost CMOS electrodes for extracellular biosensing with neuronal cells and to increase the corrosion resistance in cell culture media.

Nanoporous alumina membranes embedded in silicon have also been employed as micromolecule testing device for primary hippocampal neurons by Prasad and Quijano. Pore sizes in this study ranged from 25 to 100 nm, and a protein coating of poly-L-lysine (PLL) was used [40]. When studying the diffusion mechanisms of the molecules glucose and immunoglobulin G (IgG) through the nanopores a pore diameter of 25 nm was found to support glucose diffusion. For IgG diffusion, larger pore sizes of 50 and 100 nm were more suitable. When the nanoporous devices were used for electrical recordings from neuronal cell cultures, the effect of IgG and glucose on the cells could be detected successfully. The AAO devices remained functional for up to 5 days, and electrical measurements showed a reproducibility of

95%, which makes the AAO chips excellent candidates for neuronal signalling.

3. Connective Tissue Cell Cultures on Nanoporous Alumina Membranes

With osteoblasts and fibroblasts being connective tissue cell types, extensive studies recently focussed on their response to nanostructured AAO substrates. Alumina ceramics have already been used for hip implants since the early 1970s [75], and since then have been studied extensively with regard to implant fracture and wear [76, 77]. Over the past decade, AAO nanopores have gained increasing importance as surface modification for bone implants with improved mechanical performance and enhanced in-growth of osteoblastic cells into the implant surface.

Popat et al. presented very promising results for the growth of human fetal osteoblasts (hFOB 1.19) on AAO with approximately 75 nm pore diameters. After 1 day in culture, they observed improved cell adhesion of hFOB compared to other substrates like glass or aluminium. Osteoblast proliferation was found to be the highest on AAO substrates after 4 days of cultivation. The production of extracellular matrix was increased after 4 weeks of culture, and the cells showed higher protein content as well. Thus, the osteoblast performance was significantly improved by AAO nanopores with 75 nm size [43].

In another study, hFOB osteoblasts responded to the AAO membrane by growing extensions into nanopores of 89 nm diameter, thus adhering tightly to the nanotopography while showing normal phenotype and morphology [44]. When monitoring primary bone marrow stromal cells (MSCs) from mice on AAO with 79 nm pore size for up to 3 weeks, a positive long-term effect of the nanopores on the MSC functionality was found. A 45% increase in cell adhesion, proliferation, and viability was measured over the first 7 days in culture. After 3 weeks, a 50% increase in extracellular matrix production compared to amorphous alumina surfaces was reported [46]. Beside, the influence of the AAO nanotopography Swan and coworkers also studied the impact of surface chemistry on osteoblastic cell cultures by covalently immobilizing the cellular adhesive peptide RGDC on AAO membranes with pore diameters of 72 nm [45]. With this surface modification they observed that RGDC did not clog the pores, allowing for improved initial adhesion of hFOB 1.19 cells after 1 day and the production of extracellular matrix after 2 days in culture. Thus, osteoblasts cultured on peptide-immobilized AAO nanopores responded to both the nanotopography and the surface chemistry. This knowledge will be of great importance for the design of future nanostructured bone implant surfaces.

Briggs et al. already coated Ti-based bone implants with a layer of aluminium, which was anodised to create nanoporous alumina with pore sizes from 160 to 200 nm. An interfacial layer of Ti oxide was deposited on the Ti implant to bond the nanoporous alumina to the implant. When aluminium films on 316L stainless steel and cobalt chrome alloy specimens were tried to be anodized, the process failed

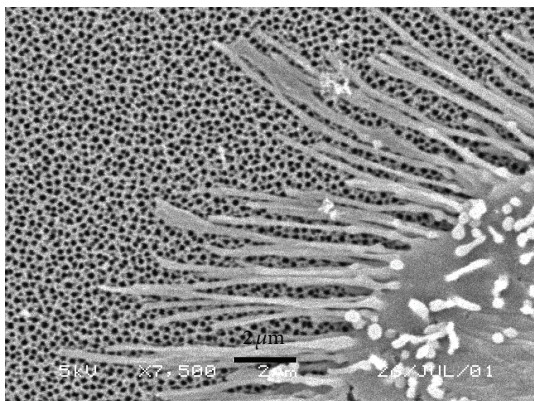


FIGURE 3: SEM micrograph of HOB cells cultured on nanoporous alumina for 24 h. Filopodia are attached tightly to the AAO nanopores and even protrude into the pores [41].

so that no nanopores were created on these surfaces [13, 14]. Studying the mechanical properties of the nanostructured Ti implant coating yielded a shear strength of up to 20.4 MPa and a tensile strength of up to 10 MPa. For comparison, the shear strength of bovine cortical bone is around 34 MPa, and for current hydroxyapatite coatings on Ti alloy surfaces it is around 12 MPa [13]. The biological performance of the AAO coatings was also found to be highly favourable, supporting normal activity of primary human osteoblast-like cells (HOB) from day 1 to 21 in cell culture. A good cell coverage was found and the osteoblastic morphology was maintained. In another study, HOB were observed to flatten on the AAO membrane with filopodia attaching well to the nanotopography and even protruding into the nanopores (see Figure 3) [41]. In these long-term cell cultures up to 2 weeks increasing cell numbers were found with a peak in cell proliferation on day 3. When the dissolution rate of AAO nanopores in cell culture medium was measured with growing cells on the nanopores no toxic effects were found. This finding suggests that the nanopores would maintain their mechanical integrity for the expected lifetime of a patient when being used *in vivo* [14].

Recently, Walpole et al. also investigated nanoporous AAO coatings on titanium substrates for implant applications. They focussed on the growth of the human osteosarcoma cell line MG63 on AAO nanopores with pore diameters from 20 to 200 nm [42]. In this study the biocompatibility of the AAO coating was found to be comparable with conventional bioinert implant materials like titanium. Furthermore, Walpole et al. introduced a new concept to improve the performance of AAO-coated bone implants with regard to bone regeneration, lower infection risks, and secured implant fixation by loading the nanopores with bioactive materials such as silica nanoparticles of different sizes (see Figure 4) [42]. Another future approach might also be to use hydroxyapatite/AAO biocomposite coatings [78].

Fibroblasts are another connective tissue cell type that has been studied on nanoporous AAO substrates. Parkinson et al. found consistent adhesion of NIH-3T3 fibroblasts on AAO nanopores with sizes from 40 to 500 nm [20]. The reaction of fibroblasts has also been investigated on AAO with

pore diameters ranging from 75 to 300 nm [47]. For NIH 3T3 fibroblasts cultured on these nanotopographies Hu et al. observed faster cell adhesion on AAO membranes of small pore sizes than on flat reference substrates. Furthermore, fibroblast adhesion and proliferation were found to increase with decreasing interpore distances. This observation correlates with the increase of focal adhesion densities of the fibroblasts. Subsequently, a microtopography was created on the AAO nanopores by bonding a PDMS layer with microholes to the membranes. Fibroblast patterning by creating geometric restraints of 50 μm diameter could be demonstrated successfully with this PDMS mask. Furthermore, it was possible to remove the PDMS mask without affecting any following treatments of the patterned cells [47].

Using photolithography, AAO membranes with 200 nm pores have also been patterned with polyethylene glycol (PEG) hydrogel microstructures to create cellular fibroblast micropatterns [48]. Thus, microwells with PEG walls and nanoporous AAO bottoms were produced with the PEG walls being nonadhesive towards the cells. The lateral well dimensions ranged from $50 \times 50 \mu\text{m}^2$ to $200 \times 200 \mu\text{m}^2$, and the PEG walls were found to crosslink with the underlying AAO nanopores. To promote fibroblast adhesion the AAO bottom was chemically modified with vitronectin, on which the cell adhesive peptide Arg-Gly-Asp (RGD) was immobilized. As a result, the fibroblasts adhered selectively to the nanoporous AAO regions and remained viable within these RGD-coated areas. For all microwell sizes filopodia of adherent cells were observed to grow into the nanopores, thus indicating an intense cell-nanopore interaction. Moreover, the morphology of cell clusters and the number of cells in one microwell depended on the lateral dimensions of the PEG wells, which enables these additional geometric features to control the behaviour of fibroblast micropatterns.

4. Growth of Epithelial Cell Cultures on Nanoporous AAO Substrates

Epithelial cells also belong to the four fundamental tissue types. To date, their proliferation and adhesion on AAO nanopores have already been the focus of many surveys, which are presented in this section.

The cultivation of human embryonic kidney cells HEK293 on AAO nanopores with extracellular matrix gel coating was previously studied by Wolfrum et al. [37]. The alumina pores had interpore distances of 30 to 200 nm and were produced on silicon substrates. For up to 14 days in culture the HEK293 cells were found to adhere and proliferate well on the alumina nanopores accompanied by normal electrophysiological performance.

Chung et al. have systematically studied the growth of epithelial normal cells (HMEC) on nanoporous AAO in dependence of the pore size and depth [50]. In their study the adhesion and proliferation of HMEC were investigated on AAO with pore sizes between 30 and 80 nm. The resulting adhesion rate of the cells did not vary for pores up to 45 nm. However, it was reduced on pores with 50 and 80 nm in diameter, which can be explained with the decreased top surface

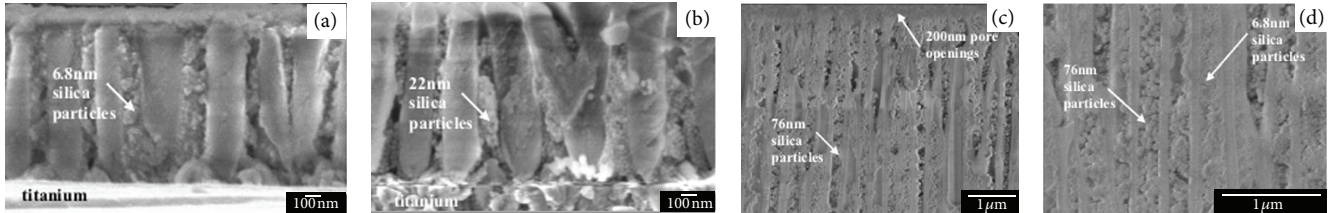


FIGURE 4: SEM images of AAO coatings with dense loading of various silica nanoparticles: (a) AAO film is 1 μm thick and loaded with 6.8 nm silica particles, (b) 1 μm thick AAO coating filled with 22 nm silica particles, (c) 60 μm thick AAO membrane loaded with 76 nm particles, and (d) 60 μm AAO film filled with simultaneous loading of 6.8 nm and 76 nm silica particles [42].

area. Successful cell proliferation was only observed on 30 nm large pores, and this phenomenon could not be explained. Furthermore, Chung et al. fabricated pore diameters of 80 nm with seven different pore depths ranging from 0 to 300 nm. It was observed that the adhesion rate of HMEC on these nanoporous AAO substrates was not influenced by the pore depth. This result was explained by the fact that the cells initially adhere to the AAO surface and then spread on top of the nanopores. Nevertheless, cell proliferation followed a different trend with a high proliferation rate on 50 and 90 nm deep pores and no cell growth on flat, 130, 180, 240, and 300 nm deep nanoporous AAO membranes. The authors explained this phenomenon by the spreading of cytoplasm into the nanoporous substrate: cells can proliferate well if the cytoplasm of the cell can spread into the nanopores and reach its bottom. However, cells which cannot reach the bottom of the nanopores have less contact with the substrate, which results in less proliferation.

Another systematic study on the interaction of endothelial cells with AAO nanopores of different depths has been carried out only recently. Thakur et al. cultivated vascular endothelial cells (ECV304) on nanoporous AAO substrates of 50 nm and 200 nm pore size with different pore depths [51]. In this survey, different cell behaviours were observed for pores with 500 nm pore depth and much deeper pores with 2000 nm pore length, respectively. On pores with 500 nm length more cell spreading was monitored, and the actin cytoskeleton appeared diffuse. This observation was independent of the pore diameter. However, when ECV304 were cultivated on the deeper pores, the cytoskeletal arrangement and the cell morphology depended on the pore size. Very prominent stress fibres formed on 50 nm pores while on pores with 200 nm diameter punctuate structures were observed. These punctuate formations indicate that the cells might protrude into the 200 nm pores with finger-like projections, which are in the range of 100 to 150 nm. Thus, in addition to the pore diameter and spacing, the pore depth is a crucial parameter for controlling cell adhesion and proliferation on AAO membranes.

Takoh et al. used the human epithelial cell line HeLa from cervix carcinoma to develop an AAO membrane-based electroporation device for localized cell stimulation and local drug delivery [52, 53]. In this setup the nanoporous AAO membrane was supported by a perforated film of the biocompatible polymer polydimethylsiloxane (PDMS), which was structured using photolithography. HeLa cells formed a

confluent monolayer on the supported AAO membranes. The cultivated substrate was then placed between two electrodes. Thus, the local delivery of ethanol was achieved through the holes in the underlying PDMS [52]. Moreover, the strength of the applied electric field could be controlled by varying the hole size in the PDMS support [53].

AAO membrane-based cell chips have also been employed recently to study the effects of anticancer drugs on the human esophageal squamous epithelial cancer cell line KYSE-30 [11, 54]. AAO membranes were prepatterned with PEG hydrogels in a photolithography approach, and the AAO bottoms were coated with the adhesion-promoting protein fibronectin, followed by the cultivation of KYSE-30 cancer cells. Good adhesion of the cancer cells was found, and the AAO nanopores were used as well controlled drug delivery system for the cancer drug cisplatin. In the diffusion study it was found that the diffusion rate of cisplatin was much larger for pore sizes of 55 nm than for pore diameters of only 25 nm [54].

The growth of the immortalized human skin cell line keratinocyte HaCaT on AAO nanopores with diameters ranging from 40 to 500 nm was studied by Parkinson et al. [20]. The keratinocytes were found to migrate fastest on nanopores with 50 nm and migrating slower on smaller pore diameters. However, the HaCaT proliferation was minimal for 125 nm pores compared to the other diameters, thus indicating that keratinocytes are sensitive to changes in the underlying nanotopography. In this study AAO membranes were used as *in vivo* wound dressings for skin repair in a pig model for the first time. Furthermore, Narayan et al. studied the growth of neonatal human epidermal keratinocytes (HEK) on AAO membranes with Pt coating and a PEG surface modification. The nanoporous substrates had diameters of 20 nm and resulted in a reduced cell viability compared to uncoated AAO membranes [55]. HEK cells were also cultivated on AAO nanopores with 20 and 100 nm diameter, which had been coated with TiO₂. Both 20 and 100 nm TiO₂-coated pores exhibited the same HEK cell viability as uncoated AAO nanopores [56]. Thus, AAO membranes with TiO₂-coatings might enable the development of future drug delivery devices, whereas the cellular response to Pt-coated AAO nanopores still needs to be studied for different pore dimensions.

When cultivating the hepatoma cell line HepG2 on self-supporting nanoporous AAO membranes with pore diameters of 70 and 260 nm, Hoess et al. found excellent cell-growth conditions [57]. For cell cultures up to 4 days *in vitro* the cells

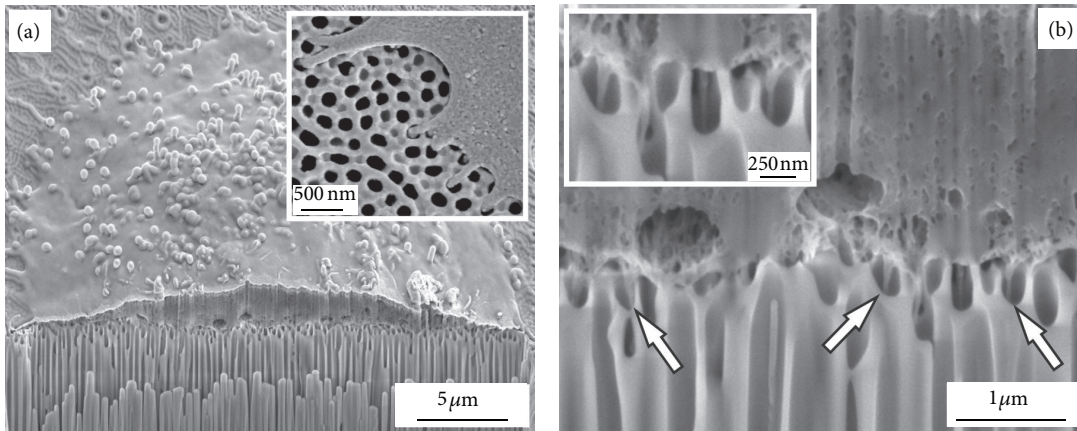


FIGURE 5: Overview (a) and magnification (b) of a FIB cross-section of a HepG2 cell cultured for 24 h on a nanoporous alumina membrane with pore diameters of 240 ± 30 nm. Inset in (a) shows the penetration of filopodia into the pores of the membrane. Inset in (b) shows a magnification of cellular protrusions extending into the pores from the cell bottom (indicated by arrows) [34].

showed good adhesion and proliferation with normal cell morphology and filopodia protruding into the larger pores with diameters >200 nm [57, 58]. This dependence of the pore diameter can be explained by the dimensions of the filopodia with diameters between 100 and 150 nm. Friedmann et al. concluded that the cells use the nanopores as anchorage points to adhere to the alumina membrane. The filopodia were even found to anchor at two different pores simultaneously, yielding an intensive cell-substrate interaction. When hepatic cell cultures on AAO membranes were extended up to 1 week and the cell-substrate interactions were studied by focussed ion beam cross-sections, the resulting images showed that the cells were connected tightly to the underlying AAO membranes without any gaps (see Figure 5). This effect was found to be independent of the pore diameter or surface roughness [59].

In addition, Hoess et al. studied the cellular interaction with mechanically stabilised AAO membranes [57]. This kind of substrate was obtained by prestructuring aluminium foil in a thermomechanical stamping process followed by anodisation, which yielded thin areas of free-standing nanopores within the supporting aluminium foil. The previous findings on self-supported AAO nanopores were confirmed. For the first time, cells were also observed to adhere to the walls of nanopores with 70 and 260 nm diameters, respectively. Based on these results, Hoess et al. developed the first self-supporting nanoporous AAO membranes for indirect cocultivation of different cell types [60]. This setup allows the cells to communicate only by diffusion of soluble mediators or growth factors through the nanopores, which can be well-controlled by adjusting the pore diameter. Primary mouse hepatocytes were cocultured with human adipose-derived mesenchymal stem cells (hASCs) on AAO membranes with pore diameters in the range of 50 to 60 nm. With this nanoporous coculture membrane, the mRNA expression of hepatogenic genes could be induced in hASCs due to the presence of mouse hepatocytes. After the cocultivation on

the nanoporous AAO membrane the two cell types could be separated easily for further studies.

Following this proof of concept, Hoess et al. studied in more detail the interaction of HepG2 cell cultures with nanoporous AAO in dependence of the pore diameter [34]. Even without any further surface modification of the membranes they found good adhesion and spreading of HepG2 cells on nanopores with diameters ranging from 50 to 250 nm. Filopodia were also observed to grow into the nanopores in this study (see inset in Figure 5(a)). Cell proliferation increased for larger pore diameters and reached its maximum on AAO membranes with 200 nm pores. Nevertheless, cell functionality, which was measured by monitoring the albumin secretion into the cell medium, increased with decreasing pore diameters down to 50 nm. Based on these results it will be possible to directly influence the response of HepG2 cells to the nanoporous coculture substrates by adjusting the pore size of the alumina membranes. In future, this will open up new approaches in the field of liver tissue engineering.

5. Muscle Cell Growth on Alumina Nanopores

To date, the growth of muscle cells on nanoporous AAO membranes has only been studied by a few groups. The reaction of smooth muscle cells (SMCs) to AAO substrates with 20 and 200 nm pore sizes was examined by Nguyen et al. They found a dependence of the cellular response from the nanotopography with regard to cell morphology and cell proliferation whereas cellular adhesion remained unchanged [63]. Cell proliferation was observed to be better on 200 nm pores than on membranes with 20 nm. Furthermore, the expression of genes involved in cell cycle, DNA replication, cell proliferation, and signalling transduction pathways was increased on the larger pores, thus demonstrating that the cellular response of SMCs strongly depends on the underlying nanopore geometry.

Ishibashi et al. used a membrane-based electroporation device with AAO pore sizes of 20 nm to electrically stimulate murine C2C12 skeletal myotubes [64]. This device, consisting of an AAO membrane on a perforated PDMS support, had previously been introduced by this group to stimulate HeLa cells [53]. With a coating of extracellular matrix (ECM) solution a confluent monolayer of myoblasts was grown on the alumina nanopores, and the cells were observed to differentiate into myotubes. When electrical current pulses of 4 mA were passed perpendicular to the myotube monolayer on the membrane, electrical stimulation of the cells was achieved. Half of the myotubes on the AAO membrane started to contract after applying the current pulses for 30 to 60 minutes. However, the stiffness of this nanoporous electroporation device was found to impede a more efficient contraction of the myotubes. To overcome this problem Kaji et al. recently developed a nanoporous electroporation device with muscle tissue-like stiffness by modifying the AAO nanopores with an atelocollagen membrane [65]. With this setup a positive correlation between the contractility of the myotubes and their glucose uptake was demonstrated.

Recently, Wesche et al. presented microelectrode arrays, which were modified with nanoporous AAO films with pore diameters below 50 nm [66]. These nanostructured cell-electrode interfaces enabled action potential recordings from cardiomyocyte HL-1 cells and also exhibited improved impedance characteristics. This result was found to originate from a nanostructuring effect of the underlying gold electrode, which occurred during the anodisation of the aluminium film. Furthermore, the HL-1 cells were found to grow in close proximity to the AAO nanopores with gaps below 100 nm. Thus, the proliferation and function of muscle cells cultivated on nanoporous AAO membranes also depend on the underlying nanotopography.

6. Blood Cell Interaction with Nanoporous AAO Membranes

The reaction of blood cells to alumina nanopores plays a critical role in the development of novel implant surfaces, which reduce the inflammatory response of the human body. Recent studies addressing this particular cell-AAO interaction are discussed in this section.

Previously, the interaction of AAO membranes with blood cells was studied by Karlsson et al. to evaluate the inflammation risk of the nanopores when being used in implants [67]. They used human neutrophils to investigate the inflammatory response to nanoporous AAO after 30 min of incubation because this cell type is one of the first cell types to encounter a foreign material such as an AAO-coated implant. In this study pore sizes of 20 and 200 nm were found to have a significant effect on the morphology and activation of the neutrophils. The 20 nm nanopores led to more extensive spreading of neutrophils with flattened morphology, which means that the cells were activated on this AAO substrate. Moreover, extended filopodia were found to establish contact with the nanoporous membrane on the 200 nm pores. On the other hand, neutrophils on 20 nm

pores showed a round shape and were thus not activated. These observations suggest that neutrophils are very sensitive to the AAO pore size and that their cellular response to nanoporous AAO surfaces can be significantly controlled by the pore diameter. In a later survey, similar results were reported for the growth of monocytes and macrophages on AAO membranes with 20 and 200 nm pore sizes [69]. Few cells with high proinflammatory activity were found on 200 nm pores whereas more but less-adherent and less-active cells were obtained on 20 nm porous alumina. These results indicate that the geometry of AAO nanopores can be used to control the inflammatory response to implants produced with this biomaterial.

The interaction of neutrophils with precoated AAO membranes was examined by Karlsson et al. In this study the alumina nanopores were incubated with human serum, fibronectin, collagen type I from calf skin, bovine serum albumin (BSA), and immunoglobulin (IgG), respectively [68]. No difference in cell morphology was found when membranes with different pore sizes precoated with the same proteins were compared. However, the fibronectin coating resulted in well-adhered neutrophils with protruding filopodia, which showed typical signs of frustrated phagocytosis. For the other coatings a round, nonactivated neutrophil morphology was observed. Thus, the activation of neutrophils can be minimized systematically by coating AAO nanopores with specific proteins. Another survey on the blood cell interaction with precoated AAO nanopores was carried out by Narayan et al. They used atomic layer deposition (ALD) to coat 20 nm pores with 8 nm platinum. The Pt-coated nanopores were subsequently modified with a PEG coating and were observed to remain free of fouling after exposure to human platelet-rich plasma [55].

To study the blood-biomaterial interaction in more detail AAO membranes of 20 and 200 nm pore size were incubated with whole blood by Ferraz et al. [70–72]. Many platelets adhered on the 20 nm pores and showed signs of activation such as spread morphology and protruding filopodia. However, only few platelets were found to adhere on the 200 nm pores [70], and this pore diameter was observed to be more complement activating than the 20 nm pores [71]. Furthermore, the procoagulant activity of the two pore sizes was compared after 60 min by measuring the release of platelet microparticles (PMP). Thus, a direct connection between nanoporosity and the PMP generation was found. Pores with diameters of 200 nm promoted PMP generation and adhesion whereas the 20 nm pores did not cause any release or adhesion of PMP. Analysing the thrombin generation, the 20 nm pores showed a 100% higher procoagulant activity than the 200 nm AAO membranes [72].

Subsequently, a time sequence study of blood activation on nanoporous AAO (20 nm and 200 nm pore size) was carried out, which ranged from 2 min incubation up to 4 hours [73]. Both AAO membranes showed similar activation time profiles up to 60 min of incubation. For longer incubation periods the platelet adhesion increased over time on the 20 nm substrate (see Figure 6) while PMP clusters on the 200 nm pores did not change. Furthermore, differences in the thrombospondin-1 (TSP-1) release were found depending on

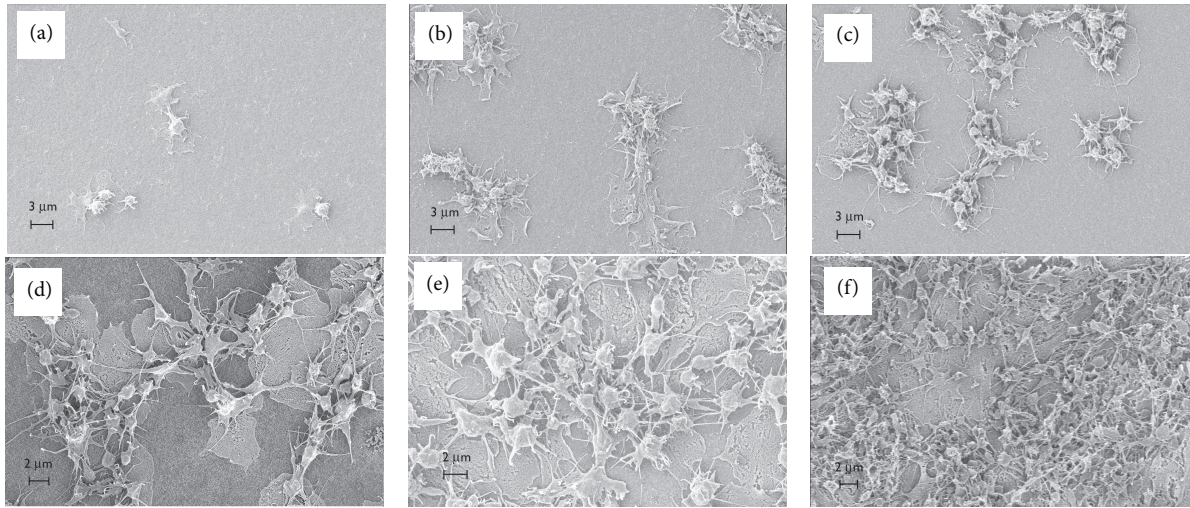


FIGURE 6: Representative SEM micrographs of 20 nm alumina membranes after 4 min (a), 8 min (b), 12 min (c), 20 min (d), 60 min (e), and 120 min (f) of whole blood incubation. The platelet adhesion pattern changes during the course of the experiment with platelet coverage becoming denser over time [73].

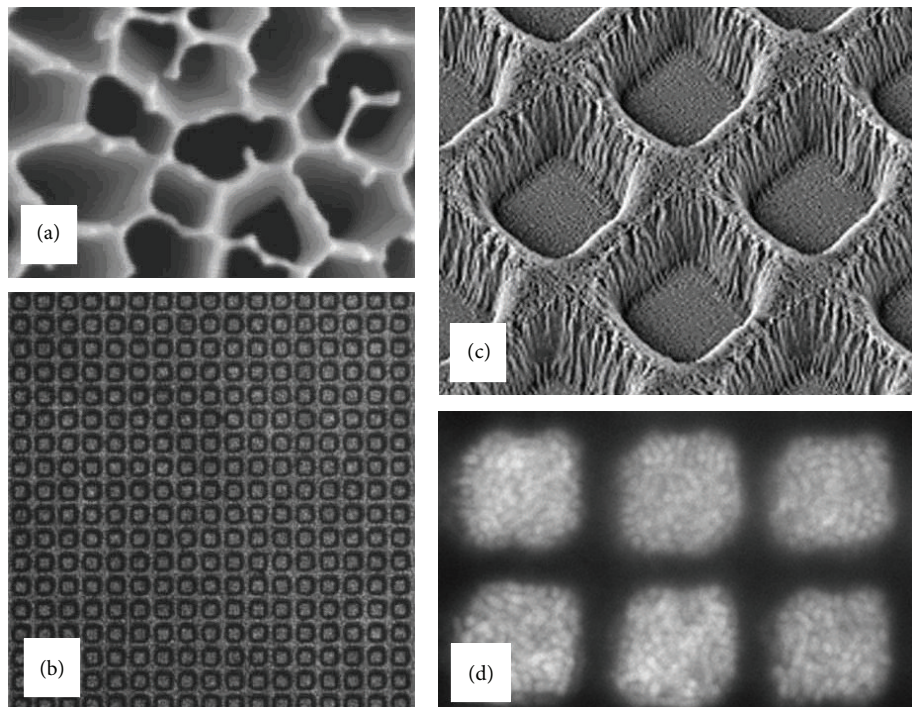


FIGURE 7: Images of growth compartments and microbial culture on AAO chips. (a) SEM of aluminium oxide showing pores on average 200 nm diameter. (b) Transmission light microscopy of hundreds of $20 \times 20 \mu\text{m}^2$ compartments viewed from above. (c) SEM image of $7 \times 7 \mu\text{m}^2$ compartments from above at a 30° angle. (d) Culture of *L. plantarum* in six compartments of the same dimensions as (c), stained with the fluorogenic dye Syto 9 after growth and imaged from above [79].

the time of incubation. TSP-1 is a protein, which mediates cell-to-cell and cell-to-matrix interactions. Its release was found to increase with time for both AAO membranes. However, the release increased much later for the 200 nm pores (240 min) than for the 20 nm pores (60 min). In a later

in vivo study Ferraz et al. implanted AAO nanopores into the peritoneal cavity of mice. Hereby, they observed that 200 nm AAO membranes induced stronger inflammatory response than 20 nm pores [74]. These findings will help to gain a better *in vivo* understanding of the events taking place in the

TABLE 2: Growth of microorganisms on prepatterned and surface-modified AAO nanopores.

Surface modification	Type of micropattern or coating on AAO nanopores	Microorganism type	Coating	Reference
Micropattern with physical barriers	(i) Commercial Anodisc AAO chips (Whatman) with 200 nm pores were coated with Ordyl 314 acrylic film (Elga Europe)	<i>Lactobacillus plantarum</i> WCFS1, <i>Escherichia coli</i> XL2 Blue, and <i>Candida albicans</i> JBZ32	Micropatterned AAO chip was cultivated on agar	[79]
	(ii) Structuring via RIE created microwells from $7 \times 7 \mu\text{m}^2$ to $150 \times 150 \mu\text{m}^2$			
	(i) Customised AAO nanopores produced via two-step anodisation (50 nm). (ii) Structuring PEG coating via photolithography yielded circular microcompartments with diameters of 80 um	<i>Escherichia coli</i> O157:H7	N/A	[80]
Cell micropatterns	(i) Commercial Anodisc chips with 200 nm pore diameter (Whatman) (ii) Contact printing of microorganisms with PDMS stamps (iii) Cells were printed on untreated and on AAO membranes compartmentalized into $40 \times 40 \mu\text{m}^2$ culture areas by acrylic plastic walls covered with a 20 nm layer of platinum	<i>Lactobacillus plantarum</i> , <i>Escherichia coli</i> , <i>Aspergillus fumigatus</i> , and several strains of <i>Candida</i>	N/A	[81, 82]
ALD deposition	(i) Commercial Anodisc nanopores with 20 and 200 nm diameter (Whatman) (ii) Coating with ZnO and TiO ₂	<i>Bacillus subtilis</i> , <i>Staphylococcus aureus</i> , <i>Escherichia coli</i> , <i>Staphylococcus epidermidis</i> , <i>Pseudomonas aeruginosa</i> , <i>Enterococcus faecalis</i> , and <i>Candida albicans</i>	N/A	[55, 56, 83]
	(i) Customised AAO nanopores with 75 nm diameter, prepared in a two-step anodisation (ii) ALD coating with Al ₂ O ₃ reduced pore size to 15 to 40 nm	<i>Phi29</i> viral particles	Customised functionalisation and polishing procedure	[84]

initial phase of implantation of AAO modified implants and will promote the development of future nanoporous implant surfaces.

7. Microorganism Cultures on Prepatterned and Surface-Modified AAO Membranes

Pre patterning approaches on nanoporous alumina membranes were recently employed by several groups to enable spatially confined growth of microorganisms on AAO nanopores. An overview on the respective works is presented in Table 2.

Ingham et al. created a disposable microbial culture chip with predefined microwells on AAO substrates of 200 nm pore diameter using photolithography (see

Figures 7(a) and 7(b)). The compartments were created by depositing an acrylic film on the AAO nanopores and subsequently opening selected areas by reactive-ion etching (RIE). Thus, up to one million growth compartments as small as $7 \times 7 \mu\text{m}^2$ were produced on the chip surface (see Figure 7(c)). With this arrangement it was shown that micro-Petri dishes can for instance be used as high-throughput screening device of microorganisms such as *Lactobacillus plantarum*, *Escherichia coli*, and *Candida albicans* (see Figure 7(d)). The prestructured AAO chips will also enable their use in viable counting systems with a high culturing efficiency [79]. Furthermore, nanoporous AAO substrates can be employed to create specific nutrient environments and oxygen limitations for cell cultures. Yu et al. also used photolithography to create PEG micropatterns on nanoporous alumina membranes with pore sizes of 50 nm. To enable good adhesion of the PEG

pattern the AAO nanopores were silanized beforehand [80]. Thus, *E. coli* bacteria were successfully patterned and captured inside the PEG microwells. With these AAO microfluidic chips the bacteria concentration effect on the impedance amplitude was explored successfully.

Another approach to create cell-patterns on AAO membranes, which was presented recently, used high-precision contact printing of the cells themselves [81]. High-density arrays of viable *C. albicans* microorganisms and spores of *A. fumigatus* were obtained on AAO nanopores with 200 nm pore size by high-precision contact printing with a PDMS stamp in a custom-modified microscope setup. AAO membranes were chosen for this cell patterning approach because they have a greater flatness and consistency than prevalent agar substrates. Furthermore, different surface modifications such as adjusting the hydrophobicity can be applied on AAO membranes, which would not be possible with agar substrates. Combining the contact printing of cells onto AAO nanopores with the previously studied fabrication of microcompartments will allow printed cells to remain segregated while growing. Recently, this work was taken further by introducing an imaging method for contact-printed microcolonies of *Candida* yeast cells on AAO membranes with 200 nm pore size [82]. With this method it was possible to reduce the time for microcolony analysis and susceptibility tests to study strain resistances. In future, such a rapid testing approach will enable the implementation of low-cost AAO-based test devices in clinical mycology.

An alternative possibility to modify the surface of AAO nanopores is the deposition of metal and metal oxide layers. Recently, Narayan et al. coated 100 nm AAO nanopores with 5 nm zinc oxide using ALD [55]. These precoated nanoporous AAO membranes demonstrated antimicrobial activity against the pathogens *Escherichia coli* and *Staphylococcus aureus*. Skoog et al. continued this antibacterial activity study for a large variety of bacteria on ZnO-coated AAO which ranged from 20 to 200 nm (see Figure 8) [83]. They observed activity of the coated AAO pores against several bacteria found on the skin surface, ranging from *Bacillus subtilis*, *Escherichia coli*, *Staphylococcus aureus* to *Staphylococcus epidermidis*. However, the zinc oxide layers did not show activity against *Pseudomonas aeruginosa*, *Enterococcus faecalis*, and *Candida albicans*. Thus, zinc oxide-coated AAO membranes can be used in several dermatologic applications like tissue coverage or cell transplantation at burn sites. In another study Narayan et al. used ALD to deposit titanium oxide (TiO_2) onto AAO membranes with pore sizes of 20 and 100 nm. These substrates were cultivated with *Staphylococcus aureus* and *Escherichia coli* [56]. In the bacteria cultures 20 nm nanoporous AAO with Ti_2O coating showed antimicrobial activity against the two microorganisms while 100 nm pores with Ti_2O did not exhibit any antimicrobial effects. These promising results suggest that ALD-modified AAO nanopores can also be used in a variety of medical and environmental health applications.

When Moon et al. used ALD of alumina films to shrink the pore size of AAO membranes from 70 nm to diameters below 40 nm they were able to capture bacteriophage phi29 virus nanoparticles on the substrates [84]. Either by chemical

surface functionalization combined with polishing or by a centrifugation process it was then possible to align the viral particles on the pores. Thus, it will also be feasible to interface viral nanoparticles with AAO nanopores in the future.

8. AAO Membranes for Immunoisolation and Drug Delivery Applications

Over the past years nanoporous alumina membranes have been introduced into several drug delivery and immunoisolation applications [3]. In 2002 biocapsules produced from AAO have been presented by Gong et al. to encapsulate molecules of different molecular weight (see Figure 9). Molecular diffusion characteristics of the AAO capsules could be well controlled for the two model drugs fluorescein and FITC dextran by adjusting the pore size from 25 to 55 nm [17]. The diffusion of molecules larger than a critical size could also be prevented in this study.

Using multiple anodisation voltages La Flamme et al. were even able to produce AAO capsules with branched pores where single branches had diameters of less than 10 nm. In a follow-up study biocapsules with pore sizes of 75 nm were found to be more durable than comparable polymeric immunoisolation designs [61]. Studying the diffusion of different molecules through these nanopores yielded good transport of glucose and insulin. On the other hand, IgG transport was impeded, which suggests that the AAO biocapsules could be used to protect cell grafts *in vivo*. When cells of the pancreatic cell line MIN6 were encapsulated in these AAO capsules for 24 hours they exhibited good viability. However, the cells were spread inhomogeneously within the capsule, which might be due to limited nutrient access in the nanoarchitecture. When various glucose stimuli were applied to the encapsulated insulin-secreting MIN6 cells they showed a dynamic response, which will enable future encapsulation strategies for the treatment of diabetes.

Further *in vitro* cytotoxicity tests with IMR-90 lung fibroblasts on AAO immunoisolation capsules have shown that the biocapsules are nontoxic [49]. *In vivo* tests were carried out by implanting untreated and PEG-coated AAO biocapsules into the peritoneal cavity of rats for up to 4 weeks. No fibrous growth was observed on any of the two capsule types after 4 weeks, and the membranes were fully intact when they were explanted. Within 1 week a moderate inflammation of the surrounding tissue was observed for PEG-modified capsules and a slightly stronger inflammation was found on pristine AAO capsules. After 4 weeks the inflammation response towards PEG-modified capsules minimized again and even blood vessels were found in the host tissue. This observation suggests that the initial inflammation response to PEG-coated AAO capsules was caused by the injury of the implantation process itself and that PEG is useful in limiting unfavourable interactions between AAO capsules and the host tissue [49]. However, unlike nanoporous biocapsules from certain polymers, AAO capsules are not biodegradable and have to be surgically removed after use [85].

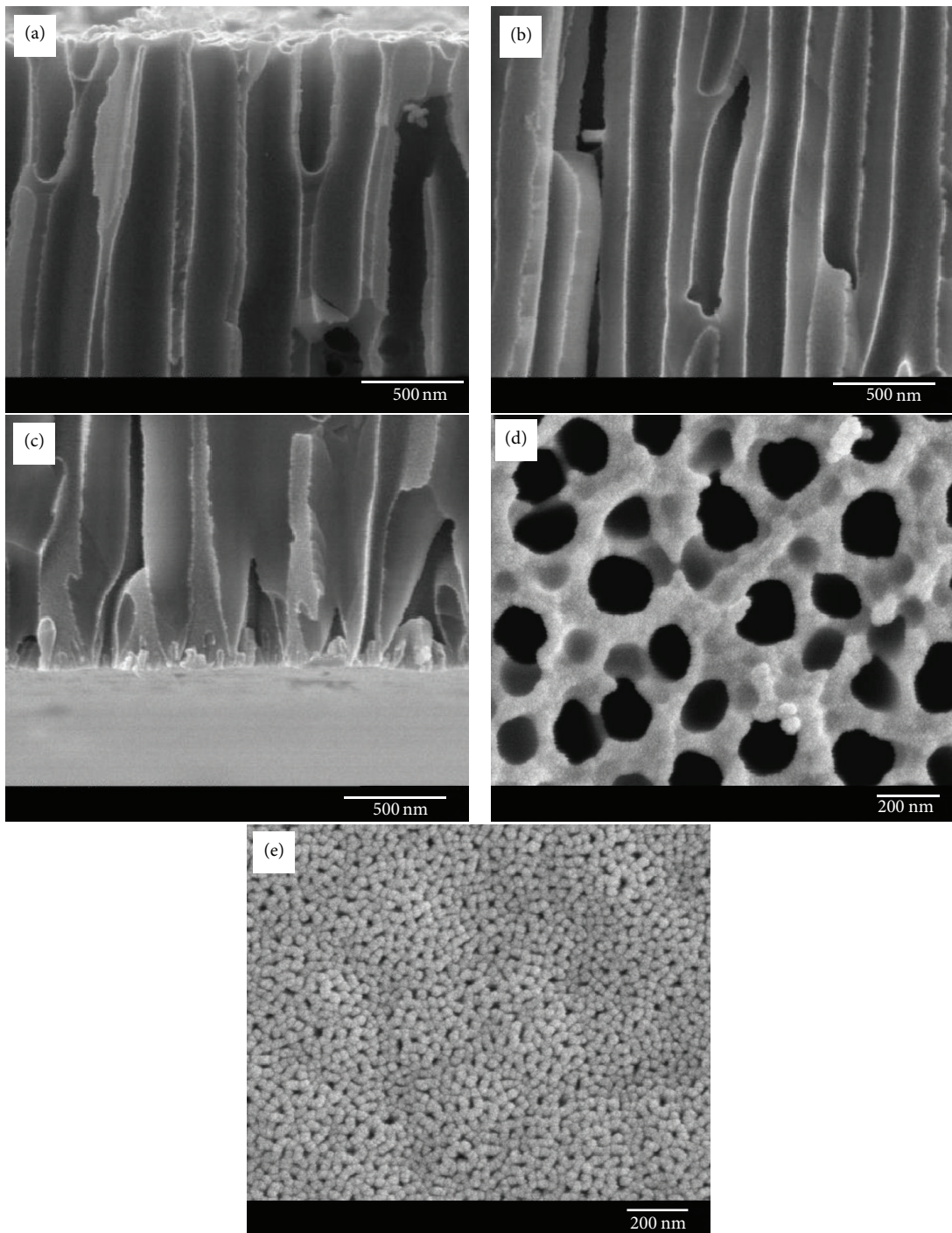


FIGURE 8: SEM images of a nanoporous AAO membrane following deposition of 8 nm zinc oxide. Cross-sectional micrographs obtained from (a) 200 nm pore diameters, (b) the middle of the pore (~100 nm), and (c) the small pore side (20 nm) of a cleaved specimen show a continuous zinc oxide coating. Plan-view scanning electron micrographs obtained from (d) the 200 nm pore side and (e) the small pore side of the membrane (20 nm) also show a continuous zinc oxide coating [83].

Recently, AAO membranes with 20 nm large pores were also presented as drug carrier for the release of amoxicillin [18]. Over 5 weeks a controlled, sustained release of the model drug was observed with an antibiotic release being proportional to the square root of time. The enzyme glucose

oxidase has also been encapsulated in AAO membranes to develop electrochemical biosensors, which measure the enzyme activity [86]. Pore sizes in this study ranged from 30 to 80 nm, and the outer surface of the biocapsule sensor was coated with the biopolymer chitosan to increase the

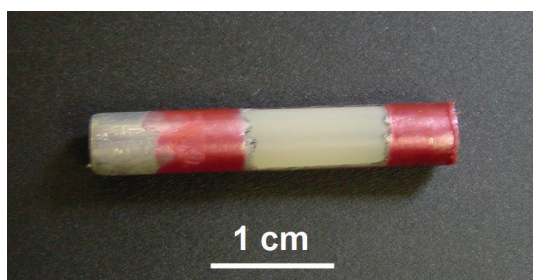


FIGURE 9: A tubular AAO capsule with silicone caps at the ends. The outside of the capsule is protected by a coating of the biopolymer chitosan. Image from Craig A. Grimes (unpublished).

enzyme stability within the capsule. When the pore diameter enhanced a larger amount of enzyme could be stored in the pores. For smaller diameters a slower response of the sensor was observed, which was the slowest for a pore diameter of 40 nm in a 150 μm thick pore.

Drug-loaded nanoporous AAO membranes have also been used as stent coatings to prevent restenosis after coronary intervention [87]. Wieneke et al. coated 316L stainless steel coronary stents with 500 nm of nanoporous AAO and loaded them with the immunosuppressive drug tacrolimus (FK506), which also inhibits the growth of human vascular smooth muscle cells [16]. The nanoporous AAO coating on its own showed good biocompatibility in the rabbit carotid artery model. Implanting drug-eluting AAO stents with FK506 in the common carotid artery of New Zealand rabbits for 28 days reduced the formation of neointima scar tissue by 50% and also yielded a lower inflammatory response by inhibiting the release of proinflammatory cytokines. When studying the *in vitro* drug release of tacrolimus from AAO-coated stents a cumulative release was measured within the first 144 hours. After 72 hours approximately 75% of the loaded drug had been eluted and 25% was still trapped in the AAO nanopores. These findings will be beneficial for the future development of nanoporous AAO stent coatings, for which further long-term investigations on the biocompatibility and the re-endothelialisation are necessary [16].

Antiangiogenic and antioxidant drugs were also loaded into capsules of AAO membranes with 20 nm pore size by Orossz et al. to study their diffusion behaviour through this nanoarchitecture [16]. They cultivated human retinal endothelial cells (HREC) on the nanomembranes and exposed them to catalase, vitamin C, and endostatin, respectively. When vitamin C diffused through the membrane it was found to modulate the HREC's ability to survive and grow. The antiangiogenic molecule endostatin could block the growth of HREC after it diffused through the AAO nanopores. Moreover, diffused catalase was able to protect the HREC culture on the AAO membrane from the cytotoxic effects of hydrogen peroxide. Thus, implantable biocapsules from AAO can also be applied in future to deliver various drugs of ophthalmic interest.

9. Summary

Nanoporous AAO membranes with highly reproducible geometries can be fabricated using an inexpensive and well-controllable etching process. Their outstanding material properties make AAO nanopores ideal candidates for biomedical applications.

To date, their interaction with a large variety of cell types has been studied extensively to understand the cellular responses to the distinct nanotopographies, which can be created with nanoporous AAO substrates. In the reviewed studies AAO nanopores were found to exhibit very good biocompatibility towards cells of the four fundamental tissue types (neuronal, epithelial, muscle, and connective tissue) as well as with blood cells and various bacteria. However, not many studies have been performed to date, which focus on muscle cells on AAO nanopores. The observed cell growth mechanisms were correlated to varying pore geometries, mostly different pore diameters. Some studies also focussed on the influence of the pore depth on cell growth. In addition, prepatterning approaches and surface modifications with metal and metal oxide coatings were introduced on AAO nanopores to enable the growth of tailored cell cultures on the nanotopographies.

From these systematic cell-AAO interfacial studies a vast range of biomedical applications has emerged. Nanoporous AAO membranes have already been incorporated into coculture substrates for tissue engineering, alumina biosensors, and bone implant coatings or nanoporous biocapsules for drug delivery. Part of these applications have also been studied *in vivo* in short-time experiments yielding promising results regarding biocompatibility, drug release properties, and mechanical stability of the nanoporous AAO membranes. A major challenge in the development of future innovative biomedical devices, which incorporate AAO nanopores as cell interfaces, will now be to study their *in vivo* response to various tissues in the long term.

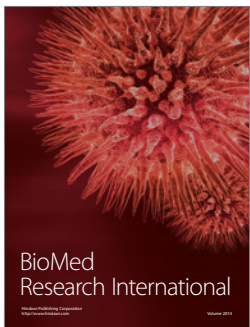
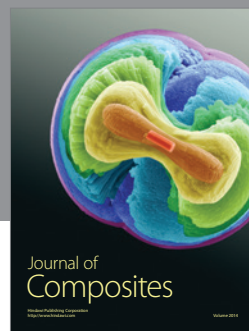
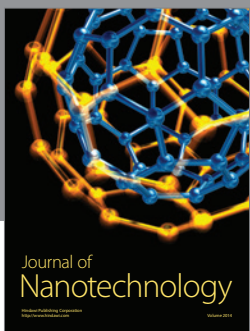
References

- [1] G. E. J. Poinern, N. Ali, and D. Fawcett, "Progress in nano-engineered anodic aluminum oxide membrane development," *Materials*, vol. 4, no. 3, pp. 487–526, 2011.
- [2] C. J. Ingham, J. ter Maat, and W. M. de Vos, "Where bio meets nano: the many uses for nanoporous aluminum oxide in biotechnology," *Biotechnology Advances*, vol. 30, no. 5, pp. 1089–1099, 2012.
- [3] E. Gultepe, D. Nagesha, S. Sridhar, and M. Amiji, "Nanoporous inorganic membranes or coatings for sustained drug delivery in implantable devices," *Advanced Drug Delivery Reviews*, vol. 62, no. 3, pp. 305–315, 2010.
- [4] A. C. Attaluri, Z. Huang, A. Belwalkar, W. van Geertruyden, D. Gao, and W. Misolek, "Evaluation of nano-porous alumina membranes for hemodialysis application," *ASAIO Journal*, vol. 55, no. 3, pp. 217–223, 2009.
- [5] S. Lee, M. Park, H. S. Park et al., "A polyethylene oxide-functionalized self-organized alumina nanochannel array for an immunoprotection biofilter," *Lab on a Chip*, vol. 11, no. 6, pp. 1049–1053, 2011.

- [6] Z. Huang, W. Zhang, J. Yu, and D. Gao, "Nanoporous alumina membranes for enhancing hemodialysis," *Journal of Medical Devices*, vol. 1, no. 1, pp. 79–83, 2007.
- [7] J. Bhattacharya, A. Kisner, A. Offenhäusser, and B. Wolfrum, "Microfluidic anodization of aluminum films for the fabrication of nanoporous lipid bilayer support structures," *Beilstein Journal of Nanotechnology*, vol. 2, no. 1, pp. 104–109, 2011.
- [8] T. Kumeria, M. D. Kurkuri, K. R. Diener, L. Parkinson, and D. Lasic, "Label-free reflectometric interference microchip biosensor based on nanoporous alumina for detection of circulating tumour cells," *Biosensors and Bioelectronics*, vol. 35, no. 1, pp. 167–173, 2012.
- [9] F. Tan, P. H. M. Leung, Z.-B. Liu et al., "A PDMS microfluidic impedance immunosensor for *E. coli* O157:H7 and *Staphylococcus aureus* detection via antibody-immobilized nanoporous membrane," *Sensors and Actuators B*, vol. 159, no. 1, pp. 328–335, 2011.
- [10] A. Kisner, R. Stockmann, M. Jansen et al., "Sensing small neurotransmitter-enzyme interaction with nanoporous gated ion-sensitive field effect transistors," *Biosensors & Bioelectronics*, vol. 31, no. 1, pp. 157–163, 2012.
- [11] J. Yu, Z. Liu, M. Yang, and A. Mak, "Nanoporous membrane-based cell chip for the study of anti-cancer drug effect of retinoic acid with impedance spectroscopy," *Talanta*, vol. 80, no. 1, pp. 189–194, 2009.
- [12] A. Heilmann, N. Teuscher, A. Kiesow, D. Janasek, and U. Spohn, "Nanoporous aluminum oxide as a novel support material for enzyme biosensors," *Journal of Nanoscience and Nanotechnology*, vol. 3, no. 5, pp. 375–379, 2003.
- [13] E. P. Briggs, A. R. Walpole, P. R. Wilshaw, M. Karlsson, and E. Pålsgård, "Formation of highly adherent nano-porous alumina on Ti-based substrates: a novel bone implant coating," *Journal of Materials Science: Materials in Medicine*, vol. 15, no. 9, pp. 1021–1029, 2004.
- [14] A. R. Walpole, E. P. Briggs, M. Karlsson, E. Pålsgård, and P. R. Wilshaw, "Nano-porous alumina coatings for improved bone implant interfaces," *Materialwissenschaft und Werkstofftechnik*, vol. 34, no. 12, pp. 1064–1068, 2003.
- [15] T. Sawitowski, W. Brandau, A. Fischer, A. Heilmann, and G. Schmid, "Nanoporous alumina coatings for medical implants and stents—radiotherapy, drug delivery, biological compatibility," *MRS Proceedings*, vol. 581, pp. 523–528, 1999.
- [16] H. Wieneke, O. Dirsch, T. Sawitowski et al., "Synergistic effects of a novel nanoporous stent coating and tacrolimus on intima proliferation in rabbits," *Catheterization and Cardiovascular Interventions*, vol. 60, no. 3, pp. 399–407, 2003.
- [17] D. Gong, V. Yadavalli, M. Paulose, M. Pishko, and C. A. Grimes, "Controlled molecular release using nanoporous alumina capsules," *Biomedical Microdevices*, vol. 5, no. 1, pp. 75–80, 2003.
- [18] K. Noh, K. S. Brammer, C. Choi et al., "A new nano-platform for drug release via nanotubular aluminum oxide," *Journal of Biomaterials and Nanobiotechnology*, vol. 2, no. 3, pp. 226–233, 2011.
- [19] L. Li, Z. Z. Zhou, Z. Li, and C. X. Wu, "Controlled drug release using nanoporous alumina capsules," *Key Engineering Materials*, vol. 361–363, pp. 1223–1226, 2008.
- [20] L. G. Parkinson, N. L. Giles, K. F. Adcroft, M. W. Fear, F. M. Wood, and G. E. Poinern, "The potential of nanoporous anodic aluminium oxide membranes to influence skin wound repair," *Tissue Engineering—Part A*, vol. 15, no. 12, pp. 3753–3763, 2009.
- [21] G. E. J. Poinern, D. Fawcett, Y. J. Ng, N. Ali, R. K. Brundavanam, and Z. T. Jiang, "Nanoengineering a biocompatible inorganic scaffold for skin wound healing," *Journal of Biomedical Nanotechnology*, vol. 6, no. 5, pp. 497–510, 2010.
- [22] G. E. J. Poinern, R. Shackleton, S. I. Mamun, and D. Fawcett, "Significance of novel bioinorganic anodic aluminum oxide nanoscaffolds for promoting cellular response," *Nanotechnology, Science and Applications*, vol. 4, no. 1, pp. 11–24, 2011.
- [23] J. J. Norman and T. A. Desai, "Methods for fabrication of nanoscale topography for tissue engineering scaffolds," *Annals of Biomedical Engineering*, vol. 34, no. 1, pp. 89–101, 2006.
- [24] D. Brüggemann, K. E. Michael, A. Wolfrum, and B. Offenhäusser, "Adhesion and survival of electrogenic cells on gold nanopillar array electrodes," *International Journal of Nano and Biomaterials*, vol. 4, no. 2, pp. 108–127, 2012.
- [25] D. Brüggemann, B. Wolfrum, V. Maybeck, Y. Mourzina, M. Jansen, and A. Offenhäusser, "Nanostructured gold microelectrodes for extracellular recording from electrogenic cells," *Nanotechnology*, vol. 22, no. 26, pp. 265104–265110, 2011.
- [26] V. A. Antohe, A. Radu, M. Mátéfi-Tempfli et al., "Nanowire-templated microelectrodes for high-sensitivity pH detection," *Applied Physics Letters*, vol. 94, no. 7, pp. 073118–073120, 2009.
- [27] J. W. Diggle, T. C. Downie, and C. W. Goulding, "Anodic oxide films on aluminum," *Chemical Reviews*, vol. 69, no. 3, pp. 365–405, 1969.
- [28] J. P. O'Sullivan and G. C. Wood, "The morphology and mechanism of formation of porous anodic films on aluminium," *Proceedings of the Royal Society of London A*, vol. 317, no. 1531, pp. 511–543, 1970.
- [29] G. D. Sulka, "Highly ordered anodic porous alumina formation by self-organized anodizing," in *Nanostructured Materials in Electrochemistry*, A. Eftekhari, Ed., pp. 1–116, Wiley-VCH, Weinheim, Germany, 2008.
- [30] D. Weber, Y. Mourzina, D. Brüggemann, and A. Offenhäusser, "Large-scale patterning of gold nanopillars in a porous anodic alumina template by replicating gold structures on a titanium barrier," *Journal of Nanoscience and Nanotechnology*, vol. 11, no. 2, pp. 1293–1296, 2011.
- [31] S. Mátéfi-Tempfli, M. Mátéfi-Tempfli, A. Vlad, V. Antohe, and L. Piroux, "Nanowires and nanostructures fabrication using template methods: a step forward to real devices combining electrochemical synthesis with lithographic techniques," *Journal of Materials Science: Materials in Electronics*, vol. 20, no. 1, pp. S249–S254, 2009.
- [32] H. B. Zhou, G. Li, X. N. Sun et al., "Integration of Au nanorods with flexible thin-film microelectrode arrays for improved neural interfaces," *Journal of Microelectromechanical Systems*, vol. 18, no. 1, pp. 88–96, 2009.
- [33] S. E. Jones, S. A. Ditner, C. Freeman, C. J. Whitaker, and M. A. Lock, "Comparison of a new inorganic membrane filter (Anopore) with a track-etched polycarbonate membrane filter (Nuclepore) for direct counting of bacteria," *Applied and Environmental Microbiology*, vol. 55, no. 2, pp. 529–530, 1989.
- [34] A. Hoess, A. Thormann, A. Friedmann, and A. Heilmann, "Self-supporting nanoporous alumina membranes as substrates for hepatic cell cultures," *Journal of Biomedical Materials Research Part A*, vol. 100, no. 9, pp. 2230–2238, 2012.
- [35] F. Haq, V. Anandan, C. Keith, and G. Zhang, "Neurite development in PC12 cells cultured on nanopillars and nanopores with sizes comparable with filopodia," *International Journal of Nanomedicine*, vol. 2, no. 1, pp. 107–115, 2007.
- [36] W. K. Cho, K. Kang, G. Kang, M. J. Jang, Y. Nam, and I. S. Choi, "Pitch-dependent acceleration of neurite outgrowth on nanosstructured anodized aluminum oxide substrates," *Angewandte*

- Chemie—International Edition*, vol. 49, no. 52, pp. 10114–10118, 2010.
- [37] B. Wolfrum, Y. Mourzina, F. Sommerhage, and A. Offenhäusser, “Suspended nanoporous membranes as interfaces for neuronal biohybrid systems,” *Nano Letters*, vol. 6, no. 3, pp. 453–457, 2006.
- [38] A. H. D. Graham, C. R. Bowen, J. Taylor, and J. Robbins, “Neuronal cell biocompatibility and adhesion to modified CMOS electrodes,” *Biomedical Microdevices*, vol. 11, no. 5, pp. 1091–1101, 2009.
- [39] A. H. D. Graham, C. R. Bowen, J. Robbins, and J. Taylor, “Formation of a porous alumina electrode as a low-cost CMOS neuronal interface,” *Sensors and Actuators B*, vol. 138, no. 1, pp. 296–303, 2009.
- [40] S. Prasad and J. Quijano, “Development of nanostructured biomedical micro-drug testing device based on *in situ* cellular activity monitoring,” *Biosensors and Bioelectronics*, vol. 21, no. 7, pp. 1219–1229, 2006.
- [41] M. Karlsson, E. Pålsgård, P. R. Wilshaw, and L. di Silvio, “Initial *in vitro* interaction of osteoblasts with nano-porous alumina,” *Biomaterials*, vol. 24, no. 18, pp. 3039–3046, 2003.
- [42] A. R. Walpole, Z. Xia, C. W. Wilson, J. T. Triffitt, and P. R. Wilshaw, “A novel nano-porous alumina biomaterial with potential for loading with bioactive materials,” *Journal of Biomedical Materials Research Part A*, vol. 90A, no. 1, pp. 46–54, 2009.
- [43] K. C. Popat, E. E. Leary Swan, V. Mukhatyar et al., “Influence of nanoporous alumina membranes on long-term osteoblast response,” *Biomaterials*, vol. 26, no. 22, pp. 4516–4522, 2005.
- [44] E. E. L. Swan, K. C. Popat, C. A. Grimes, and T. A. Desai, “Fabrication and evaluation of nanoporous alumina membranes for osteoblast culture,” *Journal of Biomedical Materials Research—Part A*, vol. 72A, no. 3, pp. 288–295, 2005.
- [45] E. E. Leary Swan, K. C. Popat, and T. A. Desai, “Peptide-immobilized nanoporous alumina membranes for enhanced osteoblast adhesion,” *Biomaterials*, vol. 26, no. 14, pp. 1969–1976, 2005.
- [46] K. C. Popat, K. I. Chalvanichkul, G. L. Barnes, T. J. Latempa, C. A. Grimes, and T. A. Desai, “Osteogenic differentiation of marrow stromal cells cultured on nanoporous alumina surfaces,” *Journal of Biomedical Materials Research—Part A*, vol. 80A, no. 4, pp. 955–964, 2007.
- [47] J. Hu, J. H. Tian, J. Shi et al., “Cell culture on AAO nanoporous substrates with and without geometry constrains,” *Microelectronic Engineering*, vol. 88, no. 8, pp. 1714–1717, 2011.
- [48] H. J. Lee, D. N. Kim, S. Park, Y. Lee, and W. G. Koh, “Micropatterning of a nanoporous alumina membrane with poly(ethylene glycol) hydrogel to create cellular micropatterns on nanotopographic substrates,” *Acta Biomaterialia*, vol. 7, no. 3, pp. 1281–1289, 2011.
- [49] K. E. La Flamme, K. C. Popat, L. Leoni et al., “Biocompatibility of nanoporous alumina membranes for immunoisolation,” *Biomaterials*, vol. 28, no. 16, pp. 2638–2645, 2007.
- [50] Z.-J. Wu, L.-P. He, and Z.-Z. Chen, “Fabrication and characterization of hydroxyapatite/Al₂O₃ biocomposite coating on titanium,” *Transactions of Nonferrous Metals Society of China (English Edition)*, vol. 16, no. 2, pp. 125104–125110, 2006.
- [51] J. Hu, J. H. Tian, J. Shi et al., “Cell culture on AAO nanoporous substrates with and without geometry constrains,” *Microelectronic Engineering*, vol. 88, no. 8, pp. 255101–255106, 2011.
- [52] K. Takoh, A. Takahashi, T. Matsue, and M. Nishizawa, “A porous membrane-based microelectroanalytical technique for evaluating locally stimulated culture cells,” *Analytica Chimica Acta*, vol. 522, no. 1, pp. 45–49, 2004.
- [53] T. Ishibashi, K. Takoh, H. Kaji, T. Abe, and M. Nishizawa, “A porous membrane-based culture substrate for localized *in situ* electroporation of adherent mammalian cells,” *Sensors and Actuators B*, vol. 128, no. 1, pp. 5–11, 2007.
- [54] Z.-B. Liu, Y. Zhang, J. J. Yu, A. F. T. Mak, Y. Li, and M. Yang, “A microfluidic chip with poly(ethylene glycol) hydrogel microarray on nanoporous alumina membrane for cell patterning and drug testing,” *Sensors and Actuators B*, vol. 143, no. 2, pp. 776–783, 2010.
- [55] R. J. Narayan, S. P. Adiga, M. J. Pellin et al., “Atomic layer deposition-based functionalization of materials for medical and environmental health applications,” *Philosophical Transactions of the Royal Society A*, vol. 368, no. 1917, pp. 2033–2064, 2010.
- [56] R. J. Narayan, N. A. Monteiro-Riviere, R. L. Brigmon, M. J. Pellin, and J. W. Elam, “Atomic layer deposition of TiO₂ thin films on nanoporous alumina templates: medical applications,” *JOM*, vol. 61, no. 6, pp. 12–16, 2009.
- [57] A. Hoess, N. Teuscher, A. Thormann, H. Aurich, and A. Heilmann, “Cultivation of hepatoma cell line HepG2 on nanoporous aluminum oxide membranes,” *Acta Biomaterialia*, vol. 3, no. 1, pp. 43–50, 2007.
- [58] A. S. Hoess, A. Staeudte, A. Thormann, M. Steinhart, and A. Heilmann, “Production of highly ordered nanoporous alumina and its application in cell cultivation,” *MRS Proceedings*, vol. 1093, pp. CC04–CC16, 2008.
- [59] A. Friedmann, A. Hoess, A. Cismak, and A. Heilmann, “Investigation of cell-substrate interactions by focused ion beam preparation and scanning electron microscopy,” *Acta Biomaterialia*, vol. 7, no. 6, pp. 2499–2507, 2011.
- [60] A. Hoess, A. Thormann, A. Friedmann, H. Aurich, and A. Heilmann, “Co-cultures of primary cells on self-supporting nanoporous alumina membranes,” *Advanced Engineering Materials*, vol. 12, no. 7, pp. B269–B275, 2010.
- [61] K. E. La Flamme, G. Mor, D. Gong et al., “Nanoporous alumina capsules for cellular macroencapsulation: transport and biocompatibility,” *Diabetes Technology and Therapeutics*, vol. 7, no. 5, pp. 684–694, 2005.
- [62] K. E. Orosz, S. Gupta, M. Hassink et al., “Delivery of antiangiogenic and antioxidant drugs of ophthalmic interest through a nanoporous inorganic filter,” *Molecular Vision*, vol. 10, no. 68, pp. 555–565, 2004.
- [63] K. T. Nguyen, K. P. Shukla, M. Moctezuma, and T. Liping, “Cellular and molecular responses of smooth muscle cells to surface nanotopography,” *Journal of Nanoscience and Nanotechnology*, vol. 7, no. 8, pp. 2823–2832, 2007.
- [64] T. Ishibashi, Y. Hoshino, H. Kaji, M. Kanzaki, M. Sato, and M. Nishizawa, “Localized electrical stimulation to C2C12 myotubes cultured on a porous membrane-based substrate,” *Biomedical Microdevices*, vol. 11, no. 2, pp. 413–419, 2009.
- [65] H. Kaji, T. Ishibashi, K. Nagamine, M. Kanzaki, and M. Nishizawa, “Electrically induced contraction of C2C12 myotubes cultured on a porous membrane-based substrate with muscle tissue-like stiffness,” *Biomaterials*, vol. 31, no. 27, pp. 6981–6986, 2010.
- [66] M. Wesche, M. Hüské, A. Yakushenko et al., “A nanoporous alumina microelectrode array for functional cell-chip coupling,” *Nanotechnology*, vol. 23, no. 49, pp. 495303–495311, 2012.
- [67] M. Karlsson, A. Johansson, L. Tang, and M. Boman, “Nanoporous aluminum oxide affects neutrophil behaviour,”

- Microscopy Research and Technique*, vol. 63, no. 5, pp. 259–265, 2004.
- [68] M. Karlsson and L. Tang, “Surface morphology and adsorbed proteins affect phagocyte responses to nano-porous alumina,” *Journal of Materials Science: Materials in Medicine*, vol. 17, no. 11, pp. 1101–1111, 2006.
- [69] N. Ferraz, J. Hong, M. Santin, and M. K. Ott, “Nanoporosity of alumina surfaces induces different patterns of activation in adhering monocytes/macrophages,” *International Journal of Biomaterials*, vol. 2010, pp. 402715–402722, 2010.
- [70] N. Ferraz, J. Carlsson, J. Hong, and M. Karlsson Ott, “Influence of nanoporesize on platelet adhesion and activation,” *Journal of Materials Science: Materials in Medicine*, vol. 19, no. 9, pp. 3115–3121, 2008.
- [71] N. Ferraz, B. Nilsson, J. Hong, and M. Karlsson Ott, “Nanopore-size affects complement activation,” *Journal of Biomedical Materials Research Part A*, vol. 87, no. 3, pp. 575–581, 2008.
- [72] N. Ferraz, J. Hong, and M. Karlsson Ott, “Procoagulant behavior and platelet microparticle generation on nanoporous alumina,” *Journal of Biomaterials Applications*, vol. 24, no. 8, pp. 675–692, 2010.
- [73] N. Ferraz, M. Karlsson Ott, and J. Hong, “Time sequence of blood activation by nanoporous alumina: studies on platelets and complement system,” *Microscopy Research and Technique*, vol. 73, no. 12, pp. 1101–1109, 2010.
- [74] N. Ferraz, A. Hoess, A. Thormann et al., “Role of alumina nanoporosity in acute cell response,” *Journal of Nanoscience and Nanotechnology*, vol. 11, no. 8, pp. 6698–6704, 2011.
- [75] P. Boutin, P. Christel, J. M. Dorlot et al., “The use of dense alumina-alumina ceramic combination in total hip replacement,” *Journal of Biomedical Materials Research*, vol. 22, no. 12, pp. 1203–1232, 1988.
- [76] T. Traykova, C. Aparicio, M. P. Ginebra, and J. A. Planell, “Bioceramics as nanomaterials,” *Nanomedicine*, vol. 1, no. 1, pp. 91–106, 2006.
- [77] T. Tateiwa, I. C. Clarke, P. A. Williams et al., “Ceramic total hip arthroplasty in the United States: safety and risk issues revisited,” *American Journal of Orthopedics*, vol. 37, no. 2, pp. E26–E31, 2008.
- [78] Z.-J. Wu, L.-P. He, and Z.-Z. Chen, “Fabrication and characterization of hydroxyapatite/ Al_2O_3 biocomposite coating on titanium,” *Transactions of Nonferrous Metals Society of China*, vol. 16, no. 2, pp. 259–266, 2006.
- [79] C. J. Ingham, A. Sprenkels, J. Bomer et al., “The micro-Petri dish, a million-well growth chip for the culture and high-throughput screening of microorganisms,” *Proceedings of the National Academy of Sciences of the United States of America*, vol. 104, no. 46, pp. 18217–18222, 2007.
- [80] S. A. Skoog, M. R. Bayati, P. E. Petrochenko et al., “Antibacterial activity of zinc oxide-coated nanoporous alumina,” *Materials Science and Engineering B*, vol. 177, no. 12, pp. e33818–e33825, 2012.
- [81] C. Ingham, J. Bomer, A. D. Sprenkels, A. van Den Berg, W. de Vos, and J. van Hylckama Vlieg, “High-resolution microcontact printing and transfer of massive arrays of microorganisms on planar and compartmentalized nanoporous aluminium oxide,” *Lab on a Chip*, vol. 10, no. 11, pp. 1410–1416, 2010.
- [82] C. J. Ingham, S. Boonstra, S. Levels, M. de Lange, J. F. Meis, and P. M. Schneeberger, “Rapid susceptibility testing and microcolony analysis of *Candida* spp. cultured and imaged on porous aluminum oxide,” *PLoS One*, vol. 7, no. 3, Article ID e33818, 2012.
- [83] S. A. Skoog, M. R. Bayati, P. E. Petrochenko et al., “Antibacterial activity of zinc oxide-coated nanoporous alumina,” *Materials Science and Engineering B*, vol. 177, no. 12, pp. 992–998, 2012.
- [84] J.-M. Moon, D. Akin, Y. Xuan, P. D. Ye, P. Guo, and R. Bashir, “Capture and alignment of phi29 viral particles in sub-40 nanometer porous alumina membranes,” *Biomedical Microdevices*, vol. 11, no. 1, pp. 135–142, 2009.
- [85] X. Zhang, H. He, C. Yen, W. Ho, and L. J. Lee, “A biodegradable, immunoprotective, dual nanoporous capsule for cell-based therapies,” *Biomaterials*, vol. 29, no. 31, pp. 4253–4259, 2008.
- [86] M. Darder, P. Aranda, M. Hernández-Vélez, E. Manova, and E. Ruiz-Hitzky, “Encapsulation of enzymes in alumina membranes of controlled pore size,” *Thin Solid Films*, vol. 495, no. 1–2, pp. 321–326, 2006.
- [87] H. Wieneke, T. Sawitowski, S. Wnendt et al., “Stent coating: a new approach in interventional cardiology,” *Herz*, vol. 27, no. 6, pp. 518–526, 2002.




Hindawi

Submit your manuscripts at
<http://www.hindawi.com>

